Journal of Hydraulic Structures
J. Hydraul. Struct., 2019; 5(2):90-106
DOI: 10.22055/jhs.2019.30450.1118

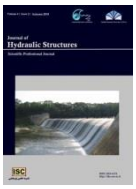

OPEN ACCESS

Determining the Uncertainty of Evaporation from Reservoir by Considering the Climate Change Conditions (Case Study: Dez Dam Reservoir)

Ali Gorjizadeh[1]
Heidar Zarei[2]
Ali Mohammad Akhoond-Ali[2]
Hesam Seyed Kaboli[3]

Abstract

Human activities have led to increased greenhouse gas emissions in the atmosphere area and it caused internal climate changes. These influences are effective on the climate parameters, which increases the temperature rate and, consequently, elevates the rate of evaporation from the free surfaces. The reservoirs of dams are influenced directly by this temperature rise as the main place of water storage, causing the annual loss of a large amount of water in them due to the evaporation phenomenon. In this research, the effect of climate change on the evaporation from Dez dam reservoir was studied considering the uncertainty of climate change scenarios. Also, the changes occurring in temperature ranges and evaporation rates in future periods were examined under climate change scenarios. The results suggested that in the coming period of 2020-2044, the annual evaporation rate will increase in all three greenhouse gas emissions scenarios, and with a probability of occurrence of 90%, the highest evaporation rate would occur in May under the A1 scenario.

Keywords: Evaporation, Climate Change, Climate Change Scenarios, Uncertainty, Dez Dam.

Received: 26 July 2018; Accepted: 12 December 2019

1. Introduction

Global warming caused by human activities (greenhouse gas emissions) has caused changes outside the range of internal climate variations in different climatic parameters such as temperature, precipitation, air humidity and solar radiation. The Fourth Report of the Intergovernmental Panel on Climate Change [1] shows that the rise of temperature in the late

[1] Department of Hydrology and Water Resources, Faculty of Water Engineering, Shahid Chamran University of Ahvaz, Ahvaz, Iran, aligorgizade@gmail.com **(Corresponding author)**
[2] Department of Hydrology and Water Resources, Faculty of Water Engineering, Shahid Chamran University of Ahvaz, Ahvaz, Iran.
[3] Faculty of Civil Engineering, Jondi-Shapour University, Dezful, Iran.

20th century has intensified in most regions. This trend is expected to continue in the 21st century. The increase in the global temperature due to climate changes has been confirmed between 1.4 and 5.8 ddegrees Celsius by 2100 [2]; therefore, this hypothesis can be true that the evaporation rate will increase in the future climate change conditions. In a study focusing on the data and information using the Magic software, Montazeri and Fahmi [3] analyzed the results obtained in different scenarios at the time horizon up to 2100. The results of climate change scenarios indicated that as the temperature rises, the evaporation will increase in most river basins throughout the year. An increase in temperature of 2 to 6 degrees Celsius causes an increase of 6% to 12% in the evaporation rate. Chattopadhyay and Hulme [4] studied the evaporation under the recent conditions and future climate changes. According to available data from recent years, it was found that the rate of evaporation has reduced; however, considering the three climate change models, it was revealed that the amount of evaporation will increase in the future. Dankers and Christensen [5] investigated the effect of climate changes on evaporation rate in the area of Tana Basin in the northern Finland and Norway. They estimated the evaporation rates due to the spatial distribution model of water balance and using the regional climate models and climate change scenarios related to the late of this century. The results showed that the evaporation rate increases during the mentioned period. Considering the effects of climate change on the Sparkling Lake in North Wisconsin in the United States, Lenters et al. [6] estimated the evaporation rate from the lake using the energy balance method through analyzing a 10-year data. The results indicated that the average evaporation rate in the studied period has had a change rate of 3.1 mm with a deviation coefficient of 25%. Donohue et al. [7] evaluated 5 formulas for estimating the potential evaporation rate under the climate change conditions. In this study, the Penman's formula presented the best value of evaporation potential rate compared to other methods. Finally, due to climate changes, it was seen that the temperature is rising followed by an increased rate of evaporation. Helfer et al. [8] evaluated the effect of climate change on the rates of temperature and evaporation from the surface of the Vinewell large reservoir in Australia for two periods, from 2030 to 2050 and from 2070 to 2090. According to the results, the surface temperature in the coming first and second periods compared to the base period from 1990 to 2010 will rise from 20.4 to 21.5 and 23.2 degrees Celsius, respectively. The evaporation rate from this reservoir will also increase by 15% in maximum rate. Yang and Yang [9] investigated the climate parameters affecting the evaporation pan rate under the conditions of climate change. In this research, the meteorological data were used from 54 stations in China from 1961 to 2001. The results suggested that the evaporation rate from the evaporation pan was 1.8% more for every decade, and the temperature rate increases by an average of 0.27 per decade. Wu et al. [10] assessed the quantitative effects of climate change and human activities in the SW basin in China. The results suggested that the evaporation rate would increase in the next period. Reshmidevi et al. [11] estimated the effects of climate change on the waterfall of the Malaprabha Basin in India. One of the results indicated an increase in the evaporation rate during the period of 2081-2100. No comprehensive study has been done in the Middle East and Iran regarding the effects of climate change on the evaporation rate from water reservoirs. Therefore, the aim of this study is to estimate the rate of evaporation from the Dez dam reservoir as one of the largest reservoirs in Iran for the incoming periods under climate change. By considering AOGCMs based on greenhouse gas emission scenarios of A1B, A2, and B1, including a total of 27 scenarios of climate change.

.

2. Methodology

2.1. Area of study

Dez dam reservoir located in Khuzestan province, has been constructed in 1961 at 25 km from Dezful city on the Dez River. The reservoir volume of Dez dam is about 3500 million cubic meters with a height of 203 meters [12]. The area of the basin is 17430 km2 with a length of 515 km [13]. Three important goals of this dam included the water supply for agricultural uses for 120,000 hectares of crop lands, the generation of 520 MWH of hydroelectric power, flood control and preventing the seasonal flooding of the Dez River. The power plant of this dam is responsible for regulating the country's (Iran) electricity frequency. Hence, the role of this dam and the need for permanent and continuous monitoring and supervision of its power plant becomes more evident than ever [12]. The study area is shown in Fig. 1.

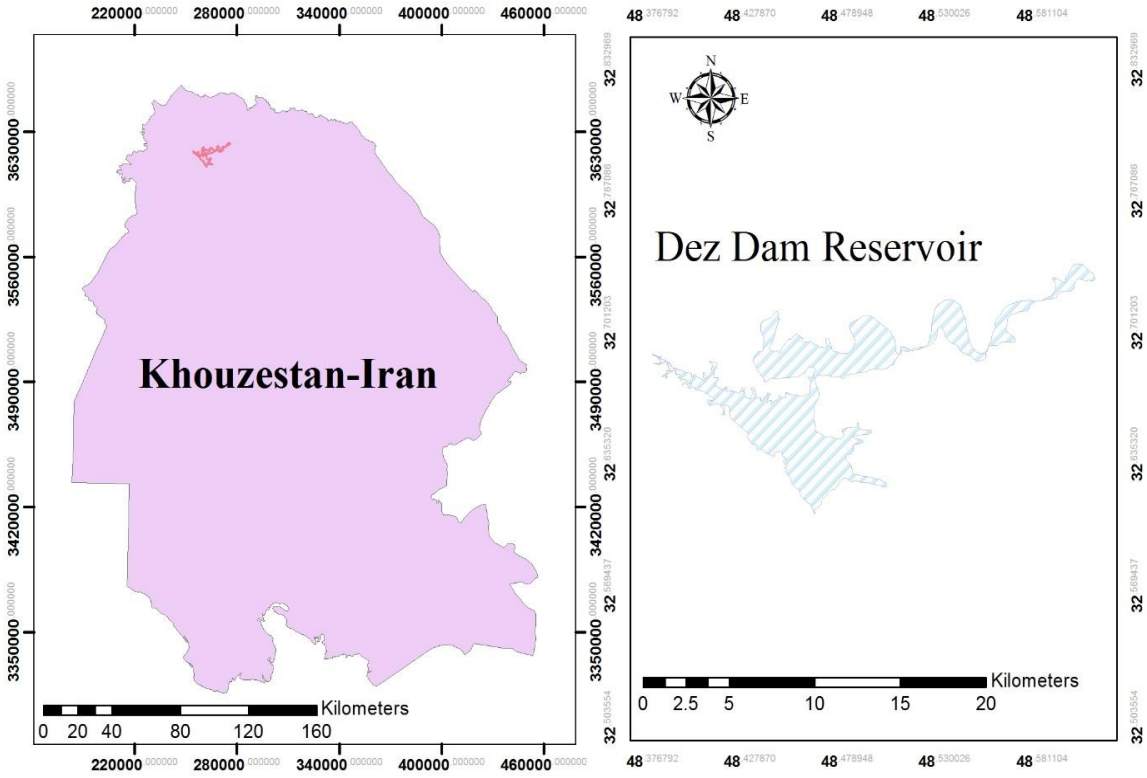

Figure 1. Study area

To determine evaporation, the best equation for estimating the evaporation rate from the water are Hamoun, Jensen-Hayes, Macking, Mayer, Rover, Priestley-Taylor, DeBruin-Kejiman and Penman methods that approaches were compared with the Energy Budget Method as the reference method [14]. The comparison results indicated that in the study area the best formula for estimating evaporation rate is the Priestley-Taylor equation [15]. This method estimates the rate of evaporation merely based on the radiation and the stored heat [15, 16].

$$E = 1.26(\Delta/(\Delta+\gamma))\,(R_{net} - S)/\lambda \quad (1)$$

$$R_{net} = \sum_{i=1}^{n}[(1-\alpha_{sw})r_{swd}(i) + (1-\alpha_{lw})r_{lwd}(i) - r_{lwu}(i)] \quad (2)$$

$$S = S_2 - S_1 = \rho_w c_w/a_{s2}\sum_{j=1}^{m_2} T_2(j)a_2(j)Z_2(j) - \rho_w c_w/a_{s2}\sum_{j=1}^{m_1} T_1(j)a_1(j)Z_1(j) \quad (3)$$

$$(\Delta/(\Delta+\gamma)) = 0.439 + 0.01124\,T_a \quad (4)$$

In the above relations,
E: Evaporation rate
$Rnet$: Net radiation
S: Change in the heat storage in the reservoir
λ: Latent heat of evaporation
αsw: Short wavelength reflection from water, with a value of 0.07
$rswd$: Downward daily short wavelength
αlw: Long wavelength reflection with a value of 0.03,
$rlwd$: Downward daily long wavelength
$rlwu$: Upward daily long wavelength
ρw: Density of water
cw: Water specific heat capacity
as: Surface area of the water in the primary and secondary periods
T: Water temperature in the intended period and depth
a: Area of water in the intended period and depth
Z: Layer thickness of the in the considered period
Ta: Air temperature

More details are given in the studies of Gorjizade et al. [15], YAO [16] and Winter et al. [17].

3. Climate Change

The IPCC has examined the future of the world in terms of distribution scenarios, considering the effects of climate change varied according to each of them. Thus, the increase rate of CO2 will rise in the incoming course according to the IPCC report. The rates of increase in 2050 under three scenarios of A1B, A2, and B1 are as the table below. It should be explained that in the implemented models for the Fifth Assessment Report (AR5), the Representative Concentration Pathways (RCP) scenarios were defined, which indicate the radiation driving [19]. Among them, the RCP 2.6 and RCP 8.5 scenarios show low emissions and radiation driving scenarios (almost consistent with scenario B1) and the high emissions and radiation driving scenarios (roughly consistent with scenarios A1 and A2), respectively. The RCP 4.5 and RCP 6 scenarios are also moderate model [18].

Table 1- CO2 increase rate in 2050*

emissions scenarios	A1B	A2	B1
Year 2050	500	500	450

*Numbers are in terms of PPMV.

In this research, the output of 10 general atmosphere-ocean circulation models under three different greenhouse gas emission scenarios were used, which in total include 27 different climatic scenarios.

The general circulation models are capable of simulating the climatic system by considering most of the processes on a global or continental scale to grid the atmosphere in three spatial directions and do the calculations at different time intervals in the nodes Masah Bavani and Morid [20]. The outputs of AOGCMs have a large spatial scale (250 to 600 km) [21], which cannot be used in studies on examining the effects of climate change [22, 23]. The micro-scaling illustrates the relationship between the output of the AOGCMs and observational data from meteorological stations [22, 24, 25]. In fact, the outputs of the general circulation models are changed by micro-scaling methods in such a way that the climate changes caused by the warming of the air can be predicted and examined on a regional scale [26]. The micro-scaling methods developed due to global climate models on a regional scale are categorized into two general dynamic and statistical micro-scaling groups. The statistical micro-scaling methods are also divided into three categories based on climatic patterns, meteorological generators approaches and the regression method [27]. In this research, the LARS-WG model was used to micro-scale the data. This model is one of the most commonly used micro-scaling methods employed in various studies (e.g., Hashmi et al. [30] Qian et al. [29] and Semenov and Barrow [28]. LARS-WG is one of the meteorological generators type. Meteorological generators are models reflecting the statistical distributions in a local climatic variable by using the mean and variance of the data. In fact, these models are random and complex generators, which outputs are meteorological data on a daily basis. The basis of this model for modeling includes the duration of dry and wet periods, daily precipitation, solar radiation series and quasi-experimental distribution [31, 32]. After calibrating the meteorological station parameters by the weather observed data at the same station, The LARS-WG model will be able to simulate the daily weather time series, which are statistically similar to the observed climate conditions. Then, through correcting the parameters by using the estimated climate change by atmosphere-ocean general circulation models, it can generate daily weather time series in the future periods [33]. In fact, the reason for choosing the LARS-WG model in this research was to model dry and wet periods, which makes it work better in estimating the precipitation parameter with having value only in the wet season and zero value on other days of the year. For micro-scaling the general atmosphere-ocean circulation models, using the LARS-WG model, the model calibration and verification were first performed (For more information see Manual et al. [31]. To this end, the daily observational data were studied, including precipitation rate and minimum and maximum temperatures collected from stations in the area. In its reports, the Pitari et al. [34] suggested the 1961-1990 period or 1971-2000 period as a desirable basic period for evaluating the climate change. In stations located in the region, due to complete information, the period of 1985-2009 was selected as the basic time. The station located at the Dez Dam site, belong to Khuzestan Water and Power Organization, was selected for micro-scaling during the statistical period.

After preparing the daily data for the period of 1985-2009 by the LARS-WG model input format, 27 different climate scenarios were made by using the output of the general circulation models for the next period of 2020-2044. Then, using these scenarios, the micro-scaling was

performed for each station individually.

Each of the AOGCMs represents a climatic scenario under any distribution scenario. Since the outputs of these models are different, the consequences of climate change in the future cannot be definitely predicted [22, 35]. Therefore, a question is always raised that which climate scenario will occur in the future by what a probability. To examine the uncertainties, the parametric and non-parametric methods are commonly used. Both methods estimate a probability density function (PDF) for a random variable [35]. This random variable can be the precipitation rate parameter or the temperature parameter obtained from climate change scenarios related to the output of the AOGCMs. By doing so, the probability of occurrence of different scenarios of climate change will be outlined in the future. In a parametric method, it is assumed that the data are from a probability distribution family like normal with unknown parameters of μ (mean) and σ2 (variance). In this case, the goal is to estimate the mean and variance parameters based on the data. In the nonparametric estimation, the density function of "f" is unknown. In this case, the data itself should determine the f-estimation [22]. In this research, to investigate the uncertainties, the nonparametric method was preferred to the parametric methods due to the low number of data. The kernel estimator, a nonparametric method, was also used. As the parameters of this distribution are unknown, these distributions are called nonparametric. The kernel estimator, with the core k, usually a symmetric density function such as Gaussian density, is defined as follows:

$$\hat{f}(x) = 1/nh \sum_{i=1}^{n} K(x - X_i)/h \quad (5)$$

Where, h, denotes window size or bandwidth, and its amount determines the level of smoothing in the kernel estimation.

4. Results & Discussion

The average temperature changes in the future relative to the base period are shown in Figs 2, 3 and 4 depending on the scenarios of distribution by considering the AOGCMs models. According to these Figs. which indicates the rare of temperature changes in the future period by considering climate change scenarios, it is determined that 9 scenarios predict a rise between 0.5 to 1 degree, 16 scenarios an increase between 1 to 1.5 degrees and 2 scenarios an increase of more than 1.5 degrees. The highest increase in the mean temperature is belong to the GISS-ER model in the A1B scenario, while the highest temperature reduction in average is related to the HADCM3 model in the B1 scenario. This result is consistent with the results presented by the IPCC. Also, according to Figs. 5, 6 and 7, indicating the evaporation changes rate in the future compared to the base period, it can be seen that 2 scenarios show evaporation changes less than zero, 9 scenarios between 0 to 1.5 mm, 14 scenarios between 1.5 to 3 mm and 2 scenarios show an increase of more than 3 millimeters. Thus, the GISS-ER-A1B scenario shows the highest evaporation rise rate, while the CSIROMk3.5-A1B scenario indicates the highest evaporation rate. The amounts of temperature and evaporation changes caused according to the scenarios of the climate change are given in Figeres 2 to 7.

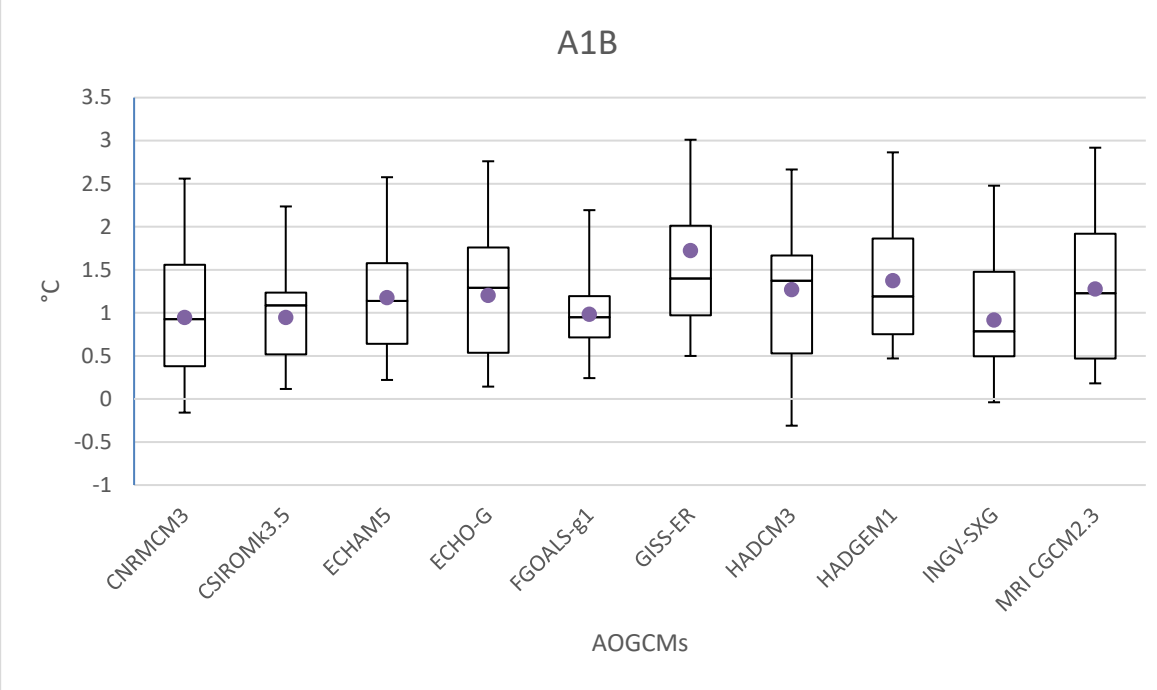

Figure 2. Temperature variations under the future climate change models by considering the A1B emission scenario.

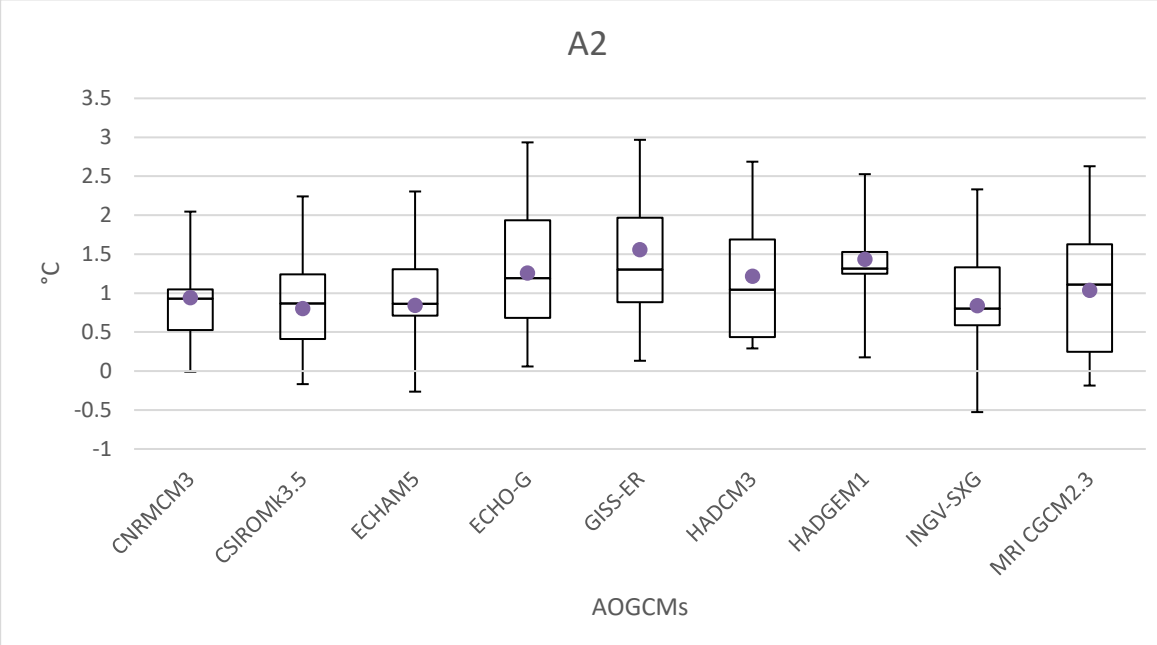

Figure 3. Temperature variations under the future climate change models by considering the A2 emission scenario

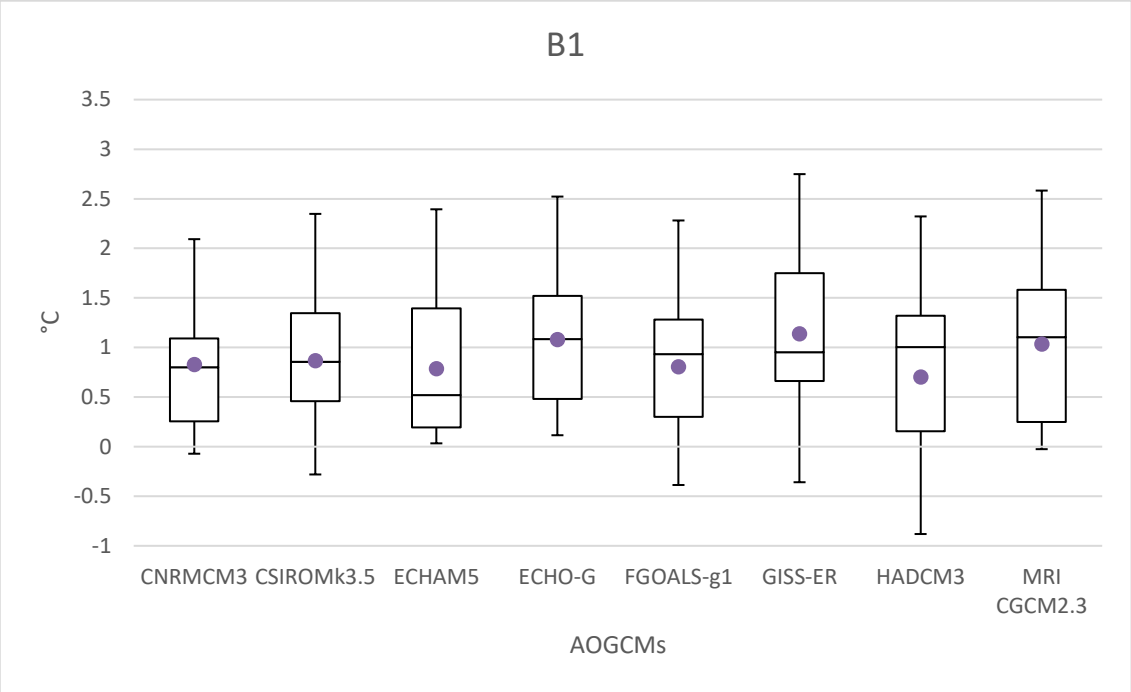

Figure 4. Temperature variations under the future climate change models by considering the B1 emission scenario

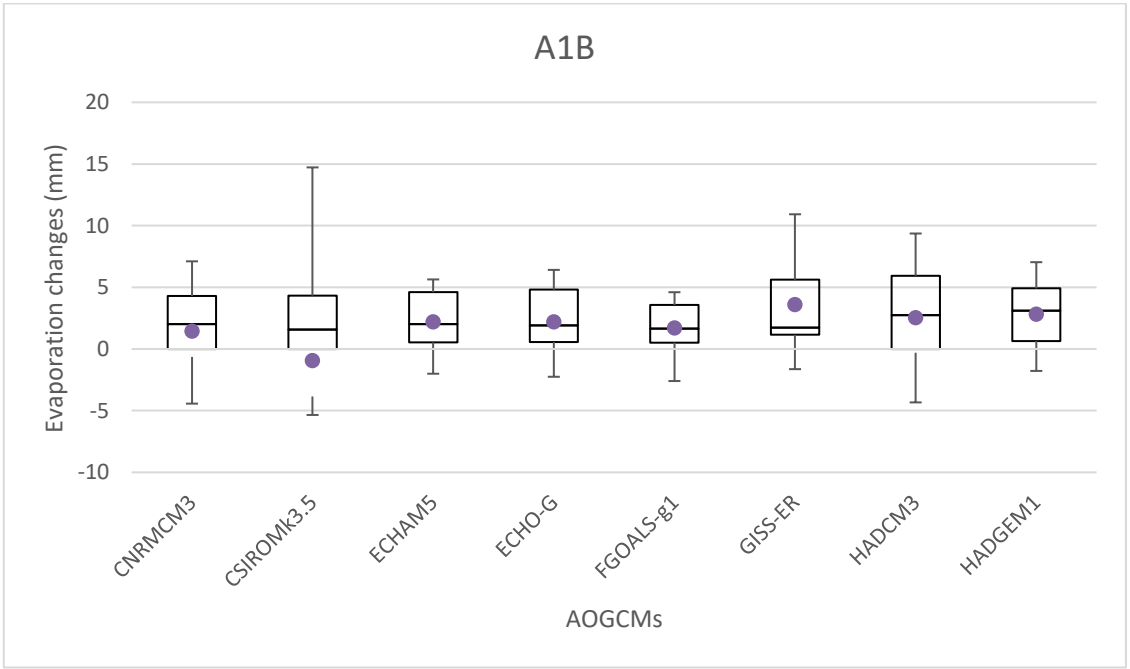

Figure 5. Evaporation variations under the future climate change models by considering the A1B emission scenario

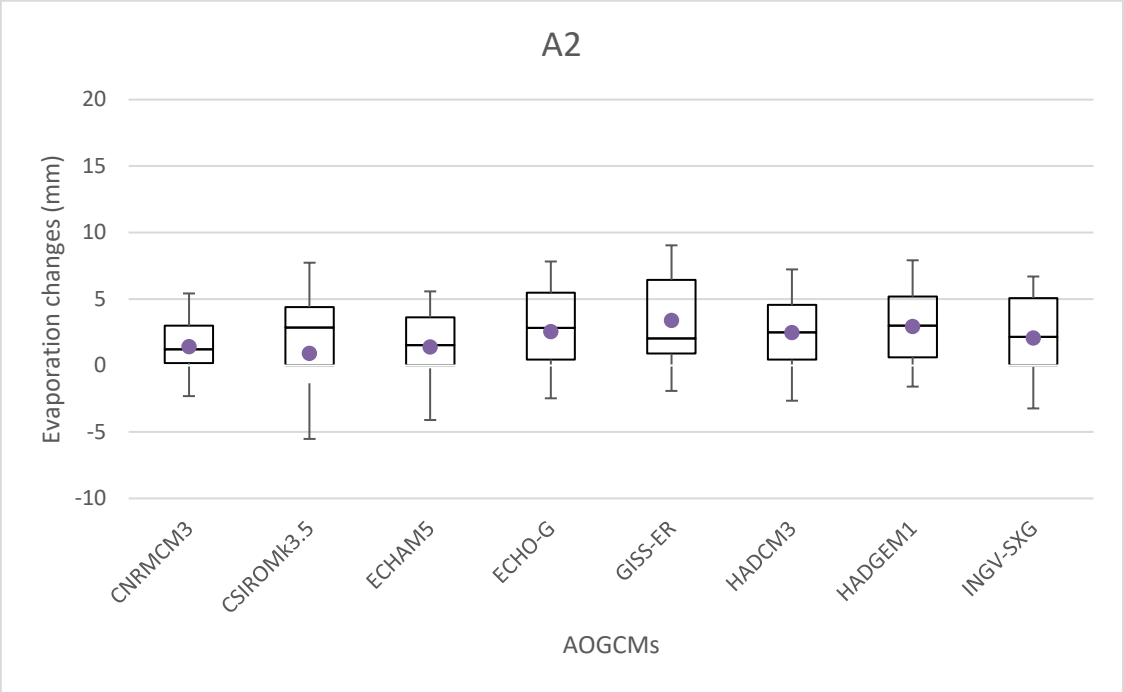

Figure 6. Evaporation variations the under future climate change models by considering the A2 emission scenario

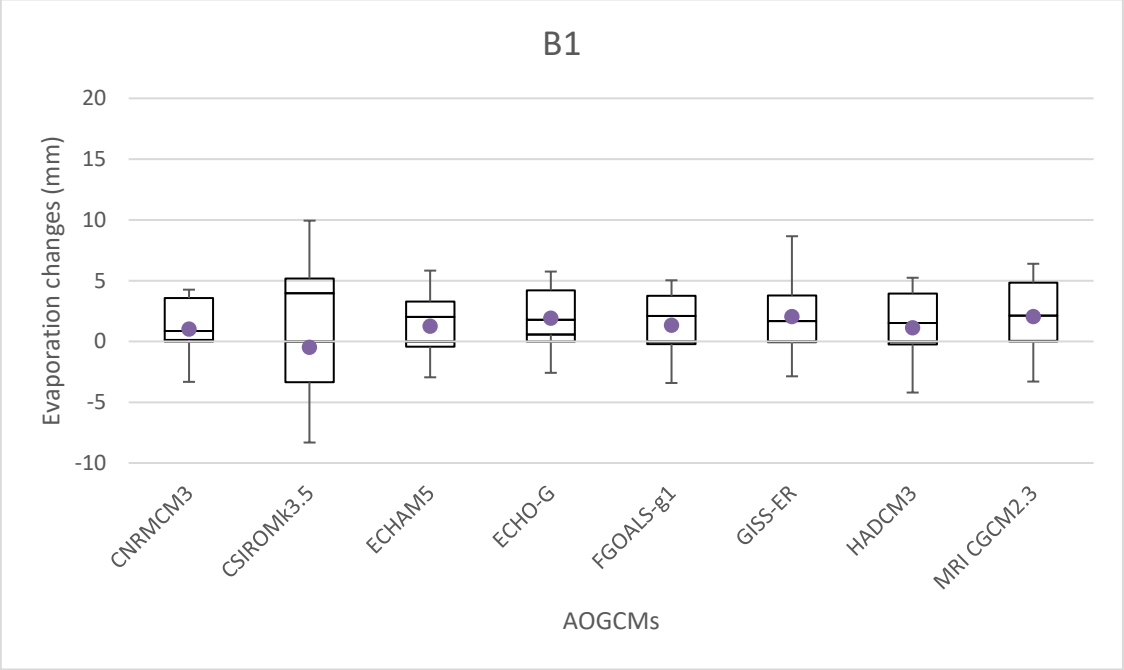

Figure 7. Evaporation variations the under future climate change models by considering the B1 emission scenario

As shown in the tables 2, the evaporation rate increases in the future in all models except for the models CSIROMk3.5-A1B and CSIROMk3.5-B1. With increased evaporation rate, the volume of the reservoir decreases, which affects the balance equation of the reservoir and reduces the hydropower production rate. This means with lower water level inside the reservoir, the production of electricity will reduce, which may affect on lives. In addition, the amount of water released for agriculture will decrease followed by a need for a change in the pattern of cultivation. This can also cause some losses in the industry sector. Also, in the environmental section, some changes will probably occur in demand for water due to increased salinity subsequent to increased evaporation rate.

The scenarios A1B and A2 have relatively similar results, but the results under scenario B1 show lower variations in the evaporation rates in the upcoming period.

According to the report provided by IPCC [34], the CO2 emission level in the emission scenario A1B is more than the A2 scenario, and in the scenario A2 more than the B1 scenario. It was also found that the estimated evaporation rate was consistent with the results of this study, suggesting that the air temperature increases with increasing greenhouse gases followed by an increase in the evaporation rate.

Given Fig. 8 the distributions with a wide range suggest that the evaporation rates vary greatly in different days, which according to equation (6) represents the higher standard deviation (S). The greater the standard deviation, the greater the error and the lower confidence in the considered scenario. As can be seen in fig. 8, in the colder months of the year, such as January and February, there are fewer variations and lower uncertainties in all three scenarios and In other months, depending on the type of greenhouse gas emission scenario, uncertainty is different for example variation range of A1B and A2 greenhouse gas emission scenarios, as a result, they have higher uncertainties while scenario B2 has less uncertainty, this could be due to the nature of the B1 scenario; Scenarios A1B and A2 indicate more use of fossil fuels in the future period, while scenario B1 indicates a reduction in fossil fuel use in the future.

$$\bar{X} - Z(S/\sqrt{n}) < \mu < \bar{X} + Z(S/\sqrt{n}) \quad (6)$$

With regard to the following figures, which show the evaporation variations versus the probability of occurrence, the probability of occurrence and the risk level of temperature and evaporation changes can be studied at any level.

Table 2- The rate of temperature variation and evaporation due to the change scenarios

Climate Change Scenario		Temperature increase (Centigrade)	Evaporation increase (mm)
CNRMCM3	-A1B	0.95	1.46
CSIROMk3.5	-A1B	0.95	-0.95
FGOALS-g1	-A1B	0.98	1.70
INGV-SXG	-A1B	0.92	1.54
CNRMCM3	-A2	0.94	1.42
CSIROMk3.5	-A2	0.80	0.91
ECHAM5	-A2	0.84	1.39
INGV-SXG	-A2	0.84	2.07
CNRMCM3	-B1	0.83	1.02
CSIROMk3.5	-B1	0.87	-0.49
ECHAM5	-B1	0.78	1.24
FGOALS-g1	-B1	0.81	1.33
HADCM3	-B1	0.70	1.12
ECHAM5	-A1B	1.18	2.20
ECHO-G	-A1B	1.20	2.19
HADCM3	-A1B	1.27	2.54
HADGEM1	-A1B	1.37	2.81
MRI CGCM2.3	-A1B	1.28	2.72
ECHO-G	-A2	1.26	2.55
HADCM3	-A2	1.21	2.47
HADGEM1	-A2	1.44	2.93
MRI CGCM2.3	-A2	1.03	1.29
ECHO-G	-B1	1.08	1.91
GISS-ER	-B1	1.14	2.06
MRI CGCM2.3	-B1	1.03	2.06
GISS-ER	-A1B	1.72	3.60
GISS-ER	-A2	1.56	3.37

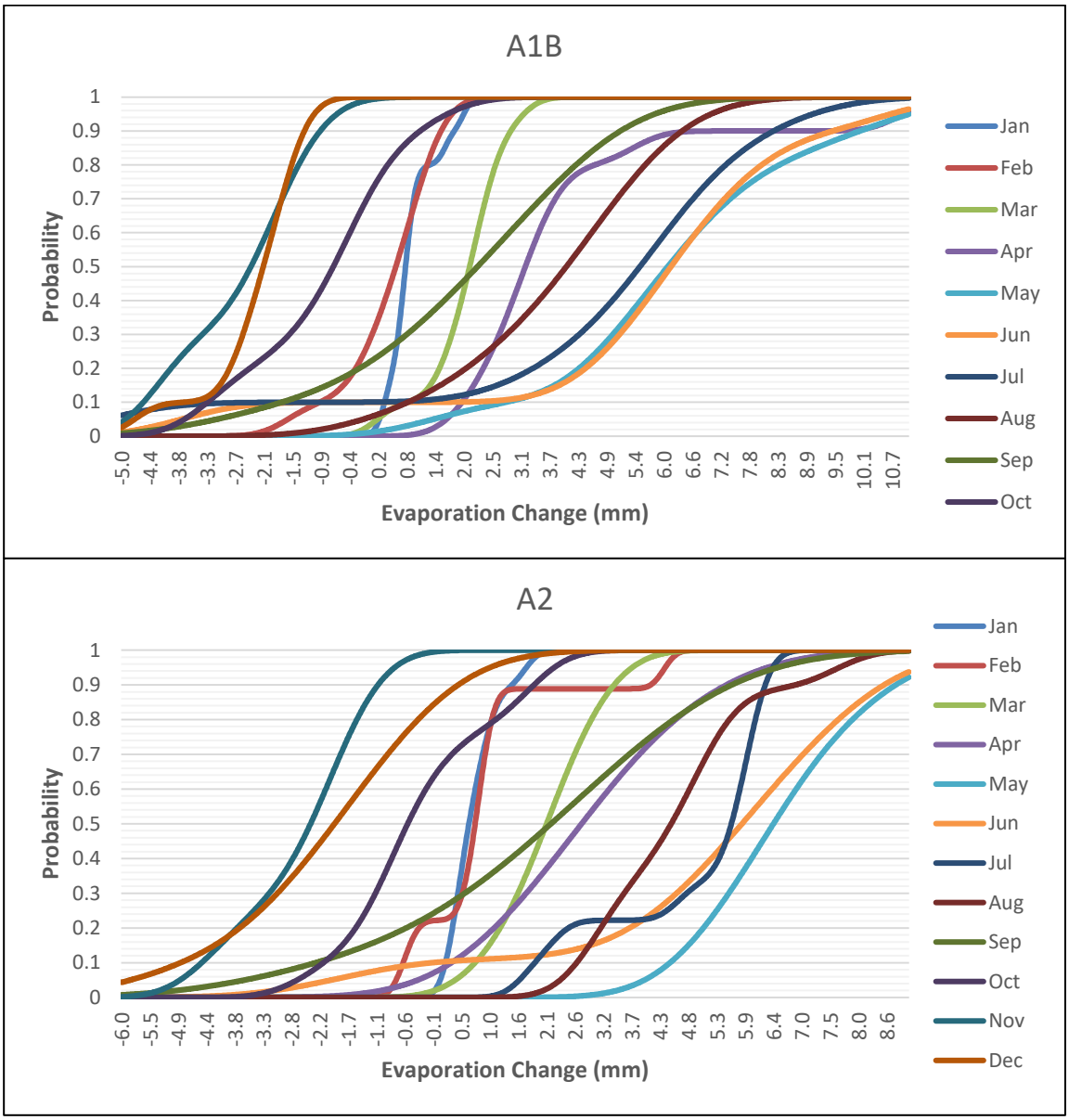
A1B
Probability
1
0.9
0.8
0.7
0.6
0.5
0.4
0.3
0.2
0.1
0
-5.0 -4.4 -3.8 -3.3 -2.7 -2.1 -1.5 -0.9 -0.4 0.2 0.8 1.4 2.0 2.5 3.1 3.7 4.3 4.9 5.4 6.0 6.6 7.2 7.8 8.3 8.9 9.5 10.1 10.7
Evaporation Change (mm)
Jan
Feb
Mar
Apr
May
Jun
Jul
Aug
Sep
Oct
A2
Probability
1
0.9
0.8
0.7
0.6
0.5
0.4
0.3
0.2
0.1
0
-6.0 -5.5 -4.9 -4.4 -3.8 -3.3 -2.8 -2.2 -1.7 -1.1 -0.6 -0.1 0.5 1.0 1.6 2.1 2.6 3.2 3.7 4.3 4.8 5.3 5.9 6.4 7.0 7.5 8.0 8.6
Evaporation Change (mm)
Jan
Feb
Mar
Apr
May
Jun
Jul
Aug
Sep
Oct
Nov
Dec

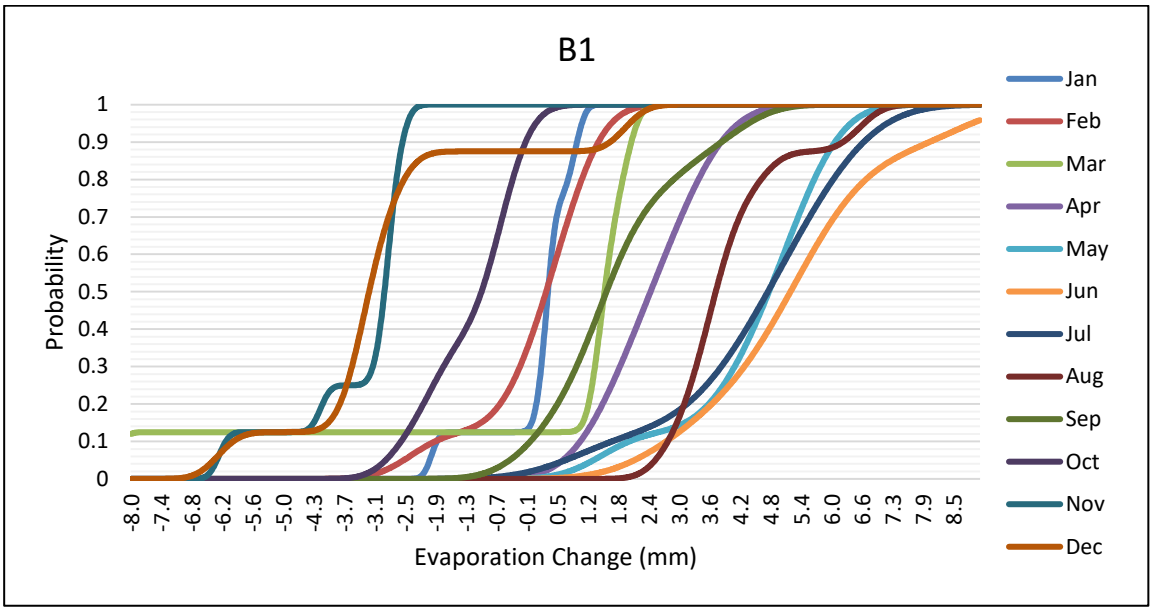

Figure 8. Uncertainty of the evaporation under climatic scenarios

Table 3- Determining the amount of monthly evaporation for future period by concidering greenhouse gas emission scenarios

Month	Probability of 10%	Probability of 50%	Probability of 90%
A1B Emission Scenario			
Jan	0.36	0.77	1.77
Feb	-0.97	0.57	1.5
Mar	0.81	2.08	2.91
Apr	1.92	3.21	7.48
May	2.81	6.1	10
Jun	0.31	6.17	9.46
Jul	-1.14	5.54	8.6
Aug	-1.43	4.04	6.4
Sep	-1.74	2.24	5.15
Oct	-3.25	-0.7	1.07
Nov	-4.55	-2.37	-0.96
Dec	-3.75	-2.12	-1.29
A2 Emission Scenario			
Jan	0.17	0.62	1.44
Feb	-0.63	0.74	4.08
Mar	0.74	2.1	3.39

Apr	0.29	2.77	5.53
May	4.45	6.43	8.76
Jun	-0.08	5.82	8.53
Jul	1.87	5.62	6.27
Aug	2.67	4.48	6.84
Sep	-2.3	2.19	5.63
Oct	-2.15	-0.55	1.86
Nov	-4.47	-2.4	-1.11
Dec	-4.87	-1.94	0.42
B1 Emission Scenario			
Jan	-1.87	0.35	0.94
Feb	-1.91	0.32	1.37
Mar	-8.5	1.49	2.03
Apr	1	2.41	3.82
May	1.98	4.78	6.1
Jun	2.72	5.21	8
Jul	1.64	4.76	6.68
Aug	2.76	3.72	6.26
Sep	0	1.53	3.83
Oct	-2.59	-0.98	-0.09
Nov	-6.1	-2.92	-2.56
Dec	-5.95	-3.23	1.6

* Negative numbers indicate a decrease in evaporation in future period.

Table 3 which results from Fig. 4, shows the probability of occurrence of evaporation changes for different months under greenhouse gas emission scenarios with three levels of 10, 50 and 90%. Considering the probability of occurrence of 10%, the maximum evaporation increase rate is related to May under scenario A2, while the highest evaporation reduction rate is in March under scenario B1. Hence, with the probability of occurrence of 50%, the highest increased evaporation rate is in June under scenario A2 and the highest reduction is related to December under scenario B1. Eventually, with 90% probability, the highest temperature rise is in May under scenario A1B and the highest temperature decrease occurs in November under scenario B1.

5. Conclusion

In this study, the evaporation rate in the future period was estimated for the next period of 2020-2044 relative to the base period of 1985-2009 by considering the scenarios of climate change. The results indicated that the evaporation rate estimated under scenarios A1B, A2, and B1 and all RCP scenarios in the upcoming period will show an increase in all seasons, except for the fall season in which we will have reduced evaporation rate. The annual evaporation rate increases in all three scenarios of greenhouse gas emissions in the next

period. The increase of evaporation is equal to 23.8 mm under the A1B scenario, 24.5 mm under A2 scenario and 15.4 mm under the scenario B1. As the surface area of the water is not available in the future period, by considering an average surface area of 60 km2, the volume of evaporated water under A1B, A2, and B1 scenarios will be respectively equal to 1.428, 1.47 and 0.924 million cubic meters, which become unavailable. This drop in the volume of the reservoir is also true under all RCP scenarios.

In addition, due to the calculated uncertainty, it was found that given the probability of occurrence of 10%, the greatest increase in evaporation is related to May under scenarios A2 and RCP 8.5, and the highest evaporation drop rate was observed in March under scenarios of B1 and RCP 2.6. Hence, with a probability of occurrence of 50%, the highest rise in the evaporation rate was observed in June under the scenarios A2 and RCP 8.5, while the highest evaporation reduction was seen in December under scenarios B1 and RCP 2.6. Finally, with the probability of occurrence of 90%, the highest increase in the evaporation rate was seen in May under the scenarios A1B and RCP 8.5, and the highest rate of evaporation reduction occurred in November under scenarios B1 and RCP 2.6.

Due to increasing evaporation in future periods and decreasing useful volume of water into the reservoir and water scarcity it is suggested to investigate the effects of climate change on Inlet runoff to dam reservoir, the rule curve and Water Allocation.

References

1. IPCC IPOCC, (2007). Climate Change 2007 - The Physical Science Basis: Working Group I Contribution to the Fourth Assessment Report of the IPCC. Science (80-). doi: volume
2. Abbasi F, Babaian I, Malboosi S et al., (2012). Assessment of Iran's climate change in the future decades (2025-2100) by using micro-scaling of general circulation of atmosphere data. Quarterly journal of geographic research pp:17979–18005.
3. Montazeri M, Fahmi H, (2003). Impacts of Climate Change on Water Resources of the Country [Iran].
4. Chattopadhyay N, Hulme M, (1997). Evaporation and potential evapotranspiration in India under conditions of recent and future climate change. Agric For Meteorol. doi: 10.1016/S0168-1923(97)00006-3
5. Dankers R, Christensen OB, (2005). Climate change impact on snow coverage, evaporation and river discharge in the sub-arctic Tana Basin, Northern Fennoscandia. Clim Change. doi: 10.1007/s10584-005-2533-y
6. Lenters JD, Kratz TK, Bowser CJ, (2005). Effects of climate variability on lake evaporation: Results from a long-term energy budget study of Sparkling Lake, northern Wisconsin (USA). J Hydrol. doi: 10.1016/j.jhydrol.2004.10.028
7. Donohue RJ, McVicar TR, Roderick ML, (2010). Assessing the ability of potential evaporation formulations to capture the dynamics in evaporative demand within a changing climate. J Hydrol. doi: 10.1016/j.jhydrol.2010.03.020
8. Helfer F, Lemckert C, Zhang H, (2012). Impacts of climate change on temperature and evaporation from a large reservoir in Australia. J Hydrol. doi: 10.1016/j.jhydrol.2012.10.008
9. Yang H, Yang D, (2012). Climatic factors influencing changing pan evaporation across

China from 1961 to 2001. J Hydrol. doi: 10.1016/j.jhydrol.2011.10.043
10. Wu L, Wang S, Bai X et al., (2017). Quantitative assessment of the impacts of climate change and human activities on runoff change in a typical karst watershed, SW China. Sci Total Environ. doi: 10.1016/j.scitotenv.2017.05.288
11. Reshmidevi T V., Nagesh Kumar D, Mehrotra R, Sharma A, (2018). Estimation of the climate change impact on a catchment water balance using an ensemble of GCMs. J Hydrol. doi: 10.1016/j.jhydrol.2017.02.016
12. Zahiri A, Shafai Bajestan M, Dehghani A, (2011). Estimation of Sediment Volume Due to Clay Flows in Dez Dam Reservoir. Journal of Water and Soil Conservation Studies 18 (1): pp:143–161.
13. Afshin Y, (1990). Rivers of iran.
14. Benzaghta MA, Mohammed TA, Ghazali AH, Soom MAM, (2012). Validation of Selected Models for Evaporation Estimation from Reservoirs Located in Arid and Semi-Arid Regions. Arabian Journal for Science and Engineering 37 (3): pp:521–534. doi: 10.1007/s13369-012-0194-5.
15. Gorjizade A, Akhondali AM, Zarei H, Kaboli HS, (2014). Evaluation of Eight Evaporation Estimation Methods in a Semi-arid Region (Dez reservoir, Iran). Int. J. Adv. Biol. Biomed. Res.
16. YAO H, (2009). Long-Term Study of Lake Evaporation and Evaluation of Seven Estimation Methods: Results from Dickie Lake, South-Central Ontario, Canada. J Water Resour Prot. doi: 10.4236/jwarp.2009.12010
17. Winter TC, Rosenberry DO, Sturrock AM, (1995). Evaluation of 11 Equations for Determining Evaporation for a Small Lake in the North Central United States. Water Resour Res. doi: 10.1029/94WR02537
18. Marengo JA, Chou SC, Torres RR et al., (2014). Climate Change in Central and South America: Recent Trends, Future Projections, and Impacts on Regional Agriculture. CGIAR Res. Progr. Clim. Chang. Agric. Food Secur.
19. Dashtbozorgi A, Aljani B, Jafarpour Z, Shakiba A, (2015). Simulation of temperature limit indices of Khuzestan province based on RCP scenarios. Geography and environmental hazards pp:301–321.
20. Masah Bavani A, Morid S, (2005). The effects of climate change on the flow of Zayandehrood River in Isfahan. Agricultural science and technology and natural resources pp:17–27.
21. Ashofte P, Masah Bavani A, (2010). Impact of Climate Change on Maximum Discharges: Case Study of Aidoghmoush Basin, East Azerbaijan. Journal of Science and Technology of Agriculture and Natural Resources 14 (53): pp:28–38.
22. Hosseinizade A, (2013). Feasibility of Impact of Future Climate Change on Groundwater Resources Considering Uncertainty Sources.
23. Ekström M, Fowler HJ, Kilsby CG, Jones PD, (2005). New estimates of future changes in extreme rainfall across the UK using regional climate model integrations. 2. Future estimates and use in impact studies. Journal of Hydrology 300 (1–4): pp:234–251. doi: 10.1016/J.JHYDROL.2004.06.019.
24. Bates BC, Charles SP, Hughes JP, (1998). Stochastic downscaling of numerical climate model simulations. Environmental Modelling & Software 13 (3–4): pp:325–331. doi: 10.1016/S1364-8152(98)00037-1.

25. Green TR, Taniguchi M, Kooi H et al., (2011). Beneath the surface of global change: Impacts of climate change on groundwater. J Hydrol. doi: 10.1016/j.jhydrol.2011.05.002
26. Barnett T, Malone R, Pennell W et al., (2004). The effects of climate change on water resources in the west: Introduction and overview. Clim Change. doi: 10.1023/B:CLIM.0000013695.21726.b8
27. Aerts JCJH, Droogers P, (2004). Climate Change in contrasting river basins. Adaptation strategies for water for food and water for the environment.
28. Semenov MA, Barrow EM, (1997). Use of a stochastic weather generator in the development of climate change scenarios. Clim Change. doi: 10.1023/A:1005342632279
29. Qian B, Gameda S, Hayhoe H, (2008). Performance of stochastic weather generators LARS-WG and AAFC-WG for reproducing daily extremes of diverse Canadian climates. Clim Res. doi: 10.3354/cr00755
30. Hashmi MZ, Shamseldin AY, Melville BW, (2011). Comparison of SDSM and LARS-WG for simulation and downscaling of extreme precipitation events in a watershed. Stoch Environ Res Risk Assess. doi: 10.1007/s00477-010-0416-x
31. Manual U, Semenov MA, Barrow EM, (2002). A Stochastic Weather Generator for Use in Climate Impact Studies. Weather
32. Babaian I, Najafi Nik Z, (2010). Analysis of Climate Change in Khorasan Razavi Province in 2010-2010 Using GCM Model Output Microprojection. Journal of Geography and Regional Development 15 pp:1–19.
33. Semenov MA, Stratonovitch P, (2010). Use of multi-model ensembles from global climate models for assessment of climate change impacts. Clim Res. doi: 10.3354/cr00836
34. Pitari G, Ackerman A, Adams P et al., (2001). Aerosols, their Direct and Indirect Effects. Clim. Chang. 2001 Sci. Basis. Contrib. Work. Gr. I to Third Assess. Rep. Intergov. Panel Clim. Chang.
35. Seyed Kaboli H, (2012). Determination of intensity, duration, and frequency curves under risk levels of climate change impacts in future periods with uncertainty sources.